Stable TiO2 nanotube arrays with high UV photo-conversion efficiency.

Francesco Mura
Department Of Chemistry Material Enviroment Engineering

Via del Castro Laurenziano 7 - 00161
Rome, Italy

Alfonso Pozio
ENEA Casaccia Research Center

Via Anguillarese 301, 00123
S.M. di Galeria (Rome), Italy

Mauro Pasquali
Department Of Chemistry Material Enviroment Engineering

Via del Castro Laurenziano 7 - 00161
Rome, Italy

Amedeo Masci
ENEA Casaccia Research Center

Via Anguillarese 301, 00123
S.M. di Galeria (Rome), Italy

ABSTRACT

This work is intended to define an optimal methodology of preparation of highly ordered TiO_2 nanotube arrays by a 60 V anodization in a glycol ethylene solution. In the order to obtain a mechanically stable structure with an high UV photoconversion efficiency is necessary to maintain a careful control of the growth mechanism by anodization process. For this reason, the nanotube arrays has to be formed upon a compact and well-defined thickness titanium dioxide layer. Besides, both fluoride concentration and anodization time are strictly correlated, because too elevated concentrations and/or a long anodization time produce instable structure with low photoconversion efficiency. The best result in the terms of reproducibility has been obtained previously operating a 3 min. galvanostatic oxide growth on the pickled titanium sheet, and anodic growth in ethylene glycol solution containing 1% wt. H_2O and 0,20% wt. NH_4F for a time lower than 4.5 hours. The UV photoconversion efficiency was measured and a maximum value of 28.3% has been obtained, which is the highest result in the literature.

Key words*:* nanotube, TiO_2, water photoelectrolysis, photoelectrode, OER

1. INTRODUCTION

T The necessity to face the global economical crisis and the alarms about climate changes has brought many important governments to stimulate investments on the energy production through renewable sources, like the solar generation of hydrogen by water photoelectolysis [1]. Titanium dioxide is regarded as the most promising photoelectrode for this application [2] and since the work published by Fujishima and Honda [3], the research on the improvement of its efficiency of this material has received an important turning point with the methodology proposed by Gong and co-workers [4]. Their article exposed a new way to obtain titania nanotube arrays via anodic oxidation of titanium foil in fluoride based solutions, which offers a remarkable simplification of the entire procedure, avoiding the presence of a template like alumina [5] or an organo-gelators [6], because the nanotube growth is produced directly on the titanium substrate.Initially, the TiO_2 anodic growth were operated in fluoride-based aqueous bath, containing electrolytes like HF [4,7], chromic acid-HF mixtures [8] and H_2SO_4-HF mixtures [9], the so-called first generation nanotubes. Than, a second generation was produced using KF or NaF electrolytes [10], but the real step forward in the growth of these nanotube arrays was made in the work of Paulose et al. [11], where they discovered the key to obtain long nanotubes, that is to minimize the water content less than 5% and to operate in polar organic solvent, like formamide, dimethyl sulfoxide [12] and ethylene glycol [13], the so-called third generation. Another important feature for these systems is that it's possible to control their morphology [14,15], length and pore size [10], and wall thickness [16], varying the three main parameters of the process: 1) the applied voltage [17,18]; 2) the time of anodization [13,19]; 3) the components and concentration of the electrolyte solutions [20,21]. Varghese et al. [22] reported the first utilization of these highly-ordered TiO_2 arrays for the water photo-electrolysis application, due to their particular geometric shape, which it's well suited for an application in water photo-electrolysis, allowing a better absorption of the incoming light and an efficient charge transfer in combination with a high surface area accessible to electrolyte percolation [1]. A very important result in terms of photoconversion efficiency values, under an UV source, was reached by K. Shankar et al. [13], obtaining a value of 16,25%. In our previous work [23], we sustained the necessity to have a fixed starting titanium dioxide layer, operating a galvanostatic treatment before the anodization growth, in order to obtain a good reproducibility. In this article, we analyze and optimize different parameters which have influence during the growth of these high-order titania nanotube arrays: the concentration of ammonium fluoride in the glycol ethylene solution in the anodization bath, the duration of the anodization process and the heat treatment. The final result is the achievement of stable and compact samples, showing very high photoconversion efficiency under UV sources respect to the higher one reported in literature [13].

1.1. Material And Photo-electrode Preparation

Little sheets of commercially pure grade 3 titanium (Titania, Italy) have been used as substrate for the nanotube growth. The samples have dimensions of 55 mm x 15 mm with a thickness of 0,5 mm, and they have been arranged to show an active area of 1 cm2. After 3 min. pickling in a HF (Carlo Erba) / HNO_3 (Carlo Erba) solution, made by a volumetric ratio of 1:3 and diluted in deionised water until to 100 ml, all the titanium sheets have been set in three-electrode cell, containing a KOH 1 M solution (Carlo Erba) and subjected to a prefixed and optimized density current (1 mA/cm_2), which is generated by a potentiostat/galvanostat Solartron 1286 for 3 min. The counter-electrode is a Platinum sheet, while the

reference is a standard calomel electrode (SCE). Then, the study of the fluoride concentration in the anodization bath has been analysed. The growth of the nanotube arrays has been operated in the system described in our previous work [23], using a Glycol Ethylene solution with 1 %wt. H_2O and 0-0.25 %wt. NH_4F for 6 h at 60 V (Tab. 1) and using an Ethylene Glycol solution with 1 %wt. H_2O and 0.20 %wt. NH_4F for a variable duration in the range of 45 min. to 6 h at fixed voltage of 60V (Tab. 2). After the anodization treatment, all the samples are washed in ethylene glycole, left overnight in the dry room, in order to dry them. So to crystallize the TiO_2 nanotubes, obtained in amorphous form by anodic growth, after a pre-heat treatment at 80°C in vacuum for 3 hours, all the samples have been placed in a tubular furnace (Lenton) for 1 h at 580°C, with a slope of 1°C/min. in air, so to be transformed into the anatase phase, which shows a higher photosensibility [24].

1.1.1. Surface Analysis

The morphology of some samples has been studied by a scanning electron microscopy analysis. The images have been obtained by a JEOL microscopy mod. JSM5510LV.

1.1.2. Measure of Photocurrent Density

The photocurrent density has been measured using a system similar to the one described by Shankar et al. [16], the entire scheme of the photo-current density has been previously described [23]. Briefly, it is made of a pyrex cell with a 1,5 cm diameter quartz window, where the light, emitted by UV source (Ultravitalux Osram) and placed at 4.5 cm of distance, moved through of it (fig. 1). This source has a spectrum with peak intensity in UVA region at 360, 400 nm. The radiation angle is 30° and the UV intensity, which is measured on the sample by a photo-Radiometer HD2302.0 (Delta OHM) over the spectral range 220-400 nm, is 13.0 mW/cm2. The active surface of the sample (1 cm2) has been immersed in a KOH 1 M solution and placed at 0.5 cm from the quartz window.

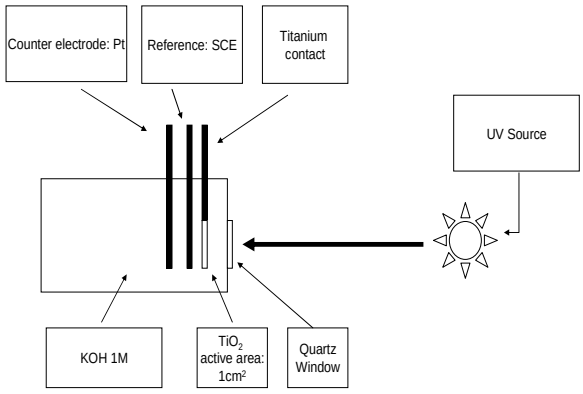

Figure 1 Scheme of photocurrent density system measure.

2. RESULTS & DISCUSSION

2.1. Analysis of fluoride concentration

In fig. 2 & 3, the anodizations (current density versus time) for samples F0÷F025 are showed (tab.1).

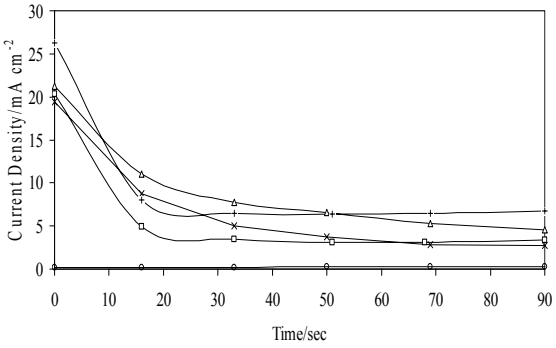

Figure 2 Current density vs. time for sample F0 (○), F01 (□), F015 (x), F020 (□), F025 (+) in the first 90 seconds of the anodization at 60 V.

Sample	Anodization Bath Composition
F0	Glycol Ethylene +1% H_2O
F01	Glycol Ethylene + 1% H_2O + 0.10 NH_4F
F015	Glycol Ethylene + 1% H_2O + 0.15 NH_4F
F020	Glycol Ethylene + 1% H_2O + 0.20 NH_4F
F025	Glycol Ethylene + 1% H_2O + 0.25 NH_4F

Tab.1 List of the titanium samples for 60 V x 6 h anodization with different bath compositions.

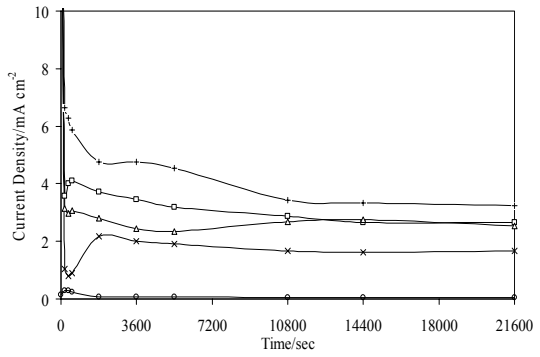

Figure 3 Current density vs. time for sample F0 (○), F01 (□), F015 (x), F020 (□), F025 (+) anodization at 60 V for 6 h.

All the curves result similar to the ones described in literature [13,25]. In the early stages of the process (fig. 1) , the rapid decrease of the current density is due to a non conductive thin oxide layer, which is formed on the surface of titanium sheet according to the following chemical reaction:

$$Ti + 2H_2O \rightarrow TiO_2 + 4H^+ + 4e^- \quad (1)$$

In presence of fluoride (samples F01÷F025), the current density at time zero has a value of about 20 mA cm^{-2} and, after 30÷50 seconds, it reaches a quasi-steady state value (2÷5 mA cm^{-2}). This constant current is due to an equilibrium between a continuous dissolution of titanium dioxide according to the following reaction and the oxidation of the metallic titanium (eq. 1) (fig. 4):

$$TiO_2 + 6F^- + 4H^+ \rightarrow TiF_6^{2-} + 2H_2O \quad (2)$$

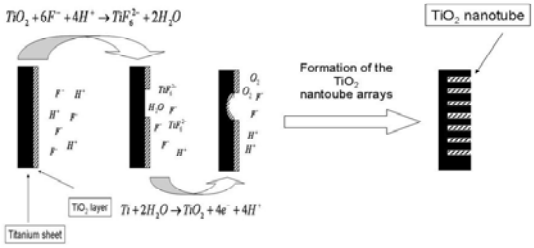

Figure 4 Scheme of the nanotube anodization growth.

According to the theory explained by Grimes et al. [1], the formation of the titania nanotube happens in this part of the anodization because of the combined processes described by eq. 1 and 2. Besides, looking at the plot of the sample F0 where we are in absence of fluoride, the current density is near to the zero which means that the presence of the F- ions in the composition of the anodization bath is absolutely necessary to active the entire process, which leads to the formation of these high-order nanotube arrays. After the heat treatment at 580 °C, the best stability of the photoelectrodes is obtained for samples produced with a fluoride concentration equal to 0.20% wt., where the amount of water is kept constant at 1% wt, while, for lower or higher NH_4F quantities, the titanium dioxide crumbles in a fine ash (F01-F015), or in the better cases, it's less adherent to the substrate (F025). The crystallization of these nanotubes is a very delicate point, the exact nature of the crystalline mixture's distribution or the crystal structure's relation to the titanium substrate is still unknown [26].

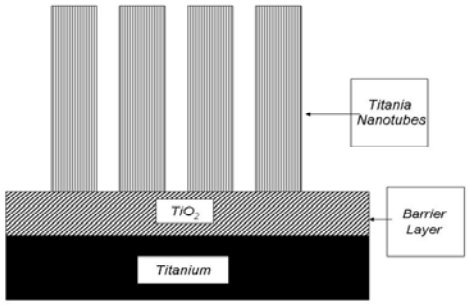

Figure 5 Scheme of the TiO2 nanotube arrays.

Looking at the fig. 5, we retain that interface Ti\TiO_2, placed under the nanotube arrays, is the key to understand why the entire system under certain conditions collapses. In fact, it's known that, for a ceramic-metal junction, operations made at high temperatures can fail if the difference in the thermal expansion coefficient is not sufficient minimized [27]. The phase transition from anatase to rutile is reported in literature to occur from 430 to 680°C [28], so it's reasonable to suppose that,

after the heat treatment at 580°C, we could have in our crystallized system both the titania forms. The tetragonal rutile or anatase crystallografic cells are characterized by different linear and volumetric thermal coefficients [23, 24]. The data, reported together with their density [29] (Tab. 2), show that anatase and rutile has the same vertical thermal expansion (αc), while this value for metallic titanium is lower. Instead, in the case of the horizontal thermal expansion (αa), the titanium expands itself almost two times more than anatase. Besides, the density of the three materials are substantially the same for rutile and titanium (4,26 g cm^{-3} vs 4,51 g cm^{-3}), while the value is lower for anatase (3.84 g cm^{-3}). So, the differences in these parameters could be the cause of the sample destruction.

	α_a (K^{-1}) [23, 24]	α_c (K^{-1}) [23,24]	β (K^{-1}) [23]	Density (g cm^{-3})
Anatase	4.47×10^{-6}	8.43×10^{-6}	17.35×10^{-6}	3.84
Rutile	7.00×10^{-6}	9.37×10^{-6}	28.68×10^{-6}	4.26
αTi	$9.5x10^{-6}$	$5.6x10^{-6}$		4.51

Tab.2 Linear (α), volumetric (β) thermal expansion coefficient and density.

To explain why the sample F020 results compact and not-ruined, we make this hypothesis: we know, from the theory exposed by Grimes et al. [1], that the fluoride/water ratio is the cause for the excavation/nanotube oxide growth on the starting titanium dioxide layer, named by the same author as "barrier layer" [1], and also that this ratio regulates the rate of the nanotube formation and the "barrier layer" thickness. Besides, the crystallization grade of the barrier layer (BL) is due to the duration and heating rate and to its thickness. Fixed the first two parameters (580°C, 1°C/min.), it will exist an optimal thickness of BL with a defined composition (anatase/rutile), which minimizes the effects due to the thermal expansion. In other words, the composition of BL obtained for a fluoride/water rate of 0.20 modifies itself after the heat treatment in a crystalline structure, made by rutile and anatase, with an average thermal expansion coefficient not very different from the one of the metallic titanium substrate.

The photocurrent density has been also measured for the only integer samples F020 and F025 and it is showed in fig. 6.

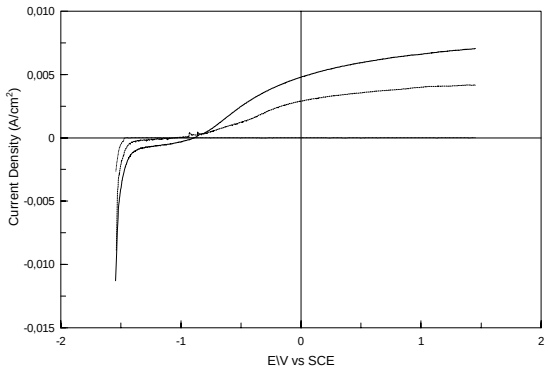

Figure 6 Photocurrent density vs. potential for sample F020 (–), F025 (— —) and dark current (- -).

We observe that the first one owns a better photocurrent density (4.8 mA/cm^2 vs 4.0 mA/cm^2 at 0V) respect to the second, while the dark currents maintain values in the range of $1*10^{-3}$ mA/cm^2. In fig. 7, the photoconversion efficiency η, which is the light energy to chemical energy conversion efficiency, is calculated for both samples with the following equation [13]:

$$\eta(\%) = j_p[(E^0_{rev} - |E_{app}|)/I_0]\times 100 \quad (3)$$

where j_p is the photocurrent density (mA/cm^2), $j_pE^0_{rev}$ is the total power output, $j_p|E_{app}|$ is the electrical power input and I_0 is the power density of incident light, which in this case is 13 mW/cm^2. E^0_{rev} is the standard reversible potential of 1.23 V/NHE. The applied potential $E_{app} = E_{meas} - E_{aoc}$, where E_{meas} is the electrode potential (vs. SCE) of the working electrode, at which photocurrent was measured under illumination. E_{aoc} is the electrode potential (vs. SCE) of the same working electrode at open circuit conditions under the same illumination and in the same electrolyte; the voltage at which the photocurrent becomes zero was taken as E_{aoc}. Even in this case, the sample F020 shows a better value (17.9% vs. 12.9%) for this parameter, meaning that a concentration

relationship between ammonium fluoride and water has to be respected, and according to these experimental data, their rate is 0.20.

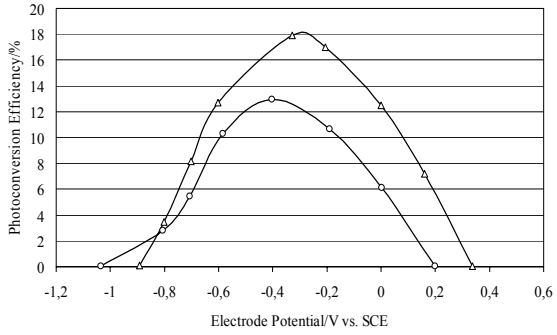

Figure 7 Photo conversion efficiency for samples F020 (Δ) and F025 (○).

2.2. Analysis of the anodization time.

In this section of article, we analyze the effect of the duration of the anodization time, keeping fixed the concentration of the electrolyte in GE-based anodization bath (0.20%wt. NH_4F, 1% H_20) and varying the time of the process from 45 to 360 min (tab. 3).

Sample	Anodization Time
H45	45 min
H90	90 min
H180	180 min
H270	270 min
H360	360 min

Table 2 – List of the titanium samples in a Glycol Ethylene + 1% H2O + 0.20 % NH4F bath for 60 V and different anodization time.

The current density plots, not reported, are broadly similar to the ones reported in Fig. 2 and 3, all of them exhibit an initial region where current density drops with a large slope, and, after a stationary or quasi-stationary phase, it reaches a final plateau. After the crystallization, each sample shows an excellent compactness and mechanical stability, confirming that the founded ratio (%wt. NH_4F/%wt. H_2O) of 0.20 overcomes the problems due to the heat treatment. In the Fig. 8÷13, we reported the side and top view SEM images for samples H45, H90 and H180.

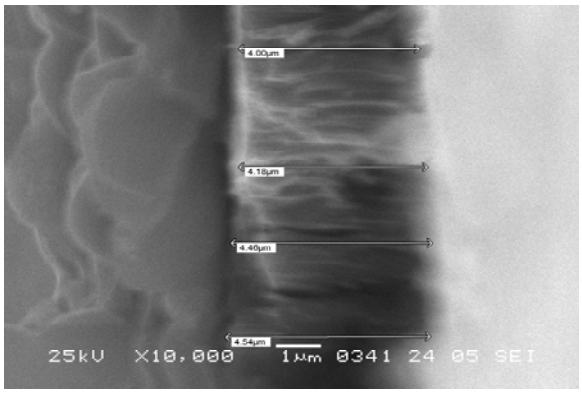

Figure 8 SEM side view for sample H45.

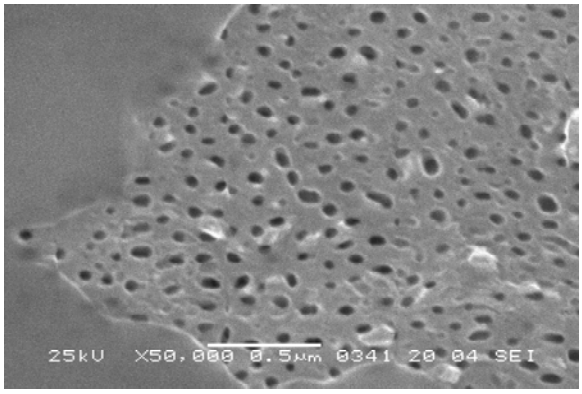

Figure 9 SEM top view for sample H45.

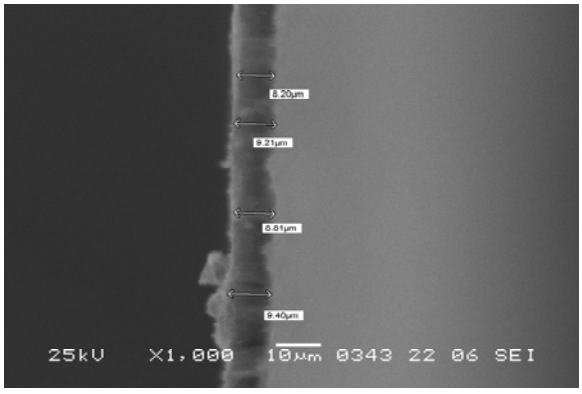

Figure 10 SEM sideview for sample H90.

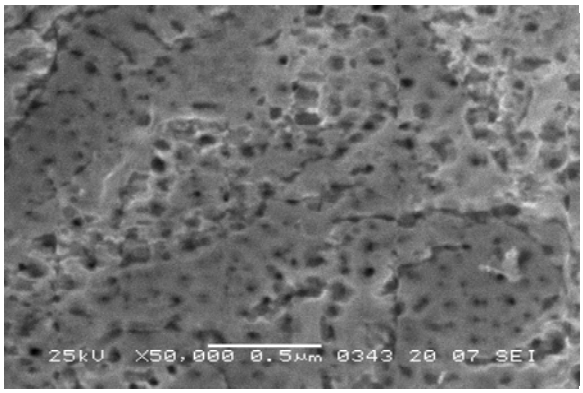

Figure 11 SEM top view for sample H90.

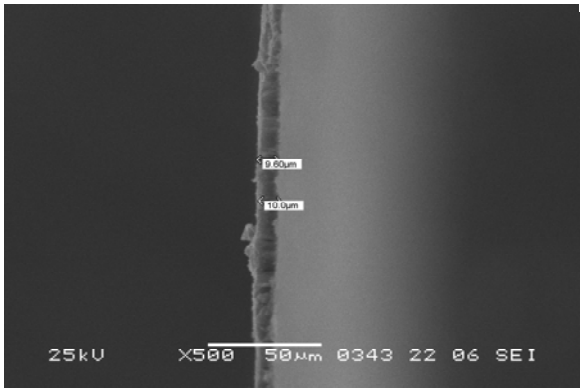

Figure 12 SEM side view for sample H180.

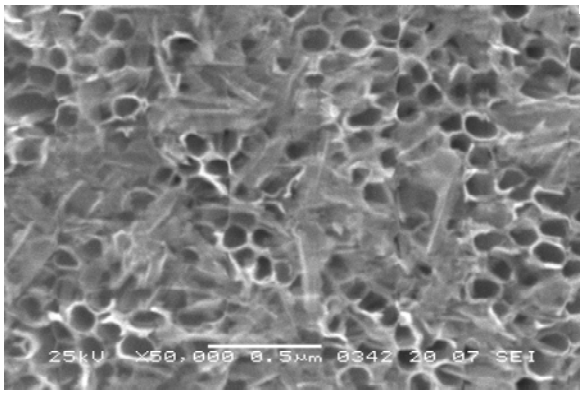

Figure 13 SEM top view for sample H180.

These photos seem to confirm the theory exposed by Grimes et al. [1] about the TiO_2 nanotubes formation. In fact, in figs. 7, 9 and 11, we notice that the nanotube length grows up from 4÷4.5 µm for an anodization of 45 minutes to about 10 µm for a 3 hours process. It's clear that the duration of the anodization is responsible for the final length of the nanotubes. This fact was already described by Shankar et al. [13]. Moreover, the figs. 8, 10 and 12 show that the nanotubes quality, in terms of surface density and average diameter, also increases with the time exactly as the Grimes model describes [1]. The photocurrent density for samples H45÷H360 is reported in fig. 13.

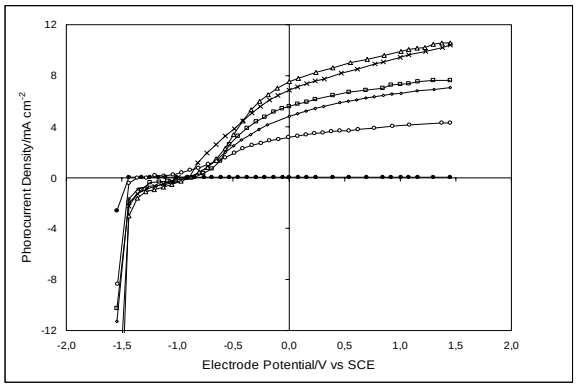

Figure 14 Photocurrent density vs. potential for sample F020 (–), F025 (— —) and dark current (- -).

It shows that the dark currents remain fixed in values in the range of $1*10^{-3}$ mA cm^{-2}, while the best value (7.7 mA cm^{-2} at 0 V) is reached by sample H180, obtained by 3 hours anodization. The high performance of this sample, as a photo-electrode, is confirmed in the fig. 14, where the plots of the UV photoconversion efficiency are calculated using the eq. 3.

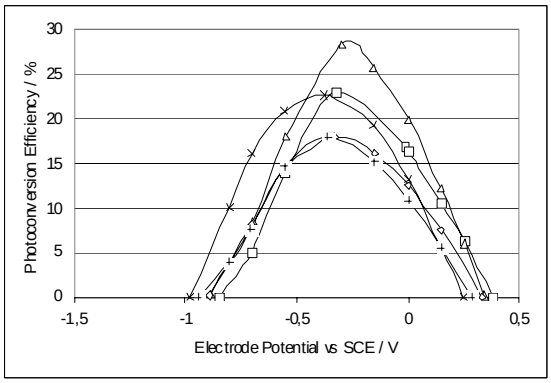

Figure 15 Photoconversion efficiency for sample H45 (x), H90 (□), H180 (Δ), H270 (+), H360 (○).

In fact, we reached a maximum efficiency of 28.3% at -0.588 V vs. SCE, which is the best result for this kind of material in literature [13]. In the same figure, we can notice how this parameter remains at high values (~22%)

for samples having an anodization time near to 3 hours, while it decreases for the other ones. This evidence was explained by Shankar et al. [13], who reported that for a too long nanotube array, the photoconversion efficiency suffers from recombination of the photogenerated electron-hole pairs.

3. CONCLUSIONS

In this article, we define an optimal methodology of preparation of highly ordered TiO_2 nanotube arrays by a 60 V anodization in a glycol ethylene solution. The nanotube arrays have to be formed upon a compact and well-defined thickness titanium dioxide layer. Besides, both fluoride concentration and anodization time are strictly correlated because elevated concentrations and/or long anodization times, which produce instable structure with low photoconversion efficiency.

The best result in terms of reproducibility has been obtained previously operating a 3 min. galvanostatic oxide growth on the pickled titanium sheet followed by an anodic growth in ethylene glycol solution containing 1% wt. H_2O and 0.20% wt. NH_4F for a time lower than 4.5 hours. Measuring the UV photoconversion efficiency, we obtained a maximum value of 28.3%, which is the highest result in the literature.

According to the model of nanotube growth [1], we tried to explain why, only for a definite fluoride\water ratio, the heat treatment does not produce any physical damage to the obtained photoelectrode. We retain that the sample degradation is probably due to the difference in the thermal expansion of the rutile\anatase barrier layer and of the metallic titanium substrate.

REFERENCES

[1]. Grimes C.A., O.K. Varghese, S. Ranjan, *"The Solar Generation Of Hydrogen By Water Photoelectrolysis"*, Springer, 2008

[2]. Bak T., J. Nowotny, M. Rekas, C.C. Sorrell, *"Photo-electrochemical properties of the TiO_2-Pt system in aqueous solutions",* Int. J. Hydrogen Energy 27, Sydney, Australia, 2002.

[3]. Fujishima A., K. Honda, .Surname Name, Name Surname, Name Surname: *"Electrochemical Photolysis Of Water At A Semiconductor Electrode"*, Nature 238, Yokohama, Japan, 1972.

[4]. Gong D., C.A. Grimes, O.K. Varghese, W. Hu, R.S. Singh, Z. Chen, E.C. Dickey, "*Titanium oxide nanotube arrays prepared by anodic oxidation"* J. Mater. Res. 16 , Pennsylvania,USA, 2001.

[5]. H. Imai, Y. Takei, K. Shimizu, M. Matsuda, H. Hirashima, *"Direct Preparation of anatase TiO2 nanotubes in porous alumina membranes"* J. Mater. Chem. 9, Yokohama, Japan, 1999.

[6]. J.H. Jung, H. Kobayashi, K.J.C. van Bommel, S. Shinkai, T. Shimizu, *"Creation of Novel Helical Ribbon and Double-Layered Nanotube TiO2 Structures Using an Organogel Template"*, Chem. Mater. 14, Tsukuba, Japan, 2002.

[7]. G.K. Mor, O.K. Varghese, M. Paulose, N. Mukherjee, C.A. Grimes, *"Fabrication of tapered, conical-shaped titania nanotubes"*, J. Mater. Res. 18, Pennsylvania,USA, 2003.

[8]. V. Zwilling, E. Darque-Ceretti, A. Bautry-Forveille, *"Anodic oxidation of titanium and TA6V alloy in chromic media. An electrochemical approach"*, Electrochim. Acta 45, Sophia-Antipolis, France, 2001.

[9]. R. Beranek, H. Hildebrand, P. Schmuki, *"Self-Organized Porous Titanium Oxide Prepared in H_2SO_4/HF Electrolytes"*, Electrochem. Solid-State Lett. 6 B12, Erlangen, Germany, 2003.

[10]. Q. Cai, M. Paulose, O.K. Varghese, C.A. Grimes, *"The effect of electrolyte composition on the fabrication of self-organized titanium oxide nanotube arrays by anodic oxidation"*, J. Mater. Res 20, Pennsylvania,USA 2005.

[11]. M. Paulose, K. Shankar, S. Yoriya, H.E. Prakasam, O.K. Varghese, G.K. Mor, T.A. Latempa, A. Fitzegerald, C.A.

Grimes, *"Anodic growth of highly ordered TiO_2 nanotube arrays to 134 μm in length"*, J. Phys. Chem. B 110, Pennsylvania, USA, 2006.

[12]. C. Ruan, M. Paulose, K. Shankar, S. Yoriya, H.E. Prakasam, O.K. Varghese, G.K. Mor, T.A. Latempa, A. Fitzegerald, C.A. Grimes, *"Fabrication of Highly Ordered TiO2 Nanotube Arrays Using an Organic Electrolyte"*, J. Phys. Chem. B 109, Pennsylvania, USA, 2005.

[13]. Shankar K., G.K. Mor, H.E. Prakasam, S. Yoriya, M. Paulose, O.K. Varghese and C.A. Grimes, *"Highly-ordered TiO_2 nanotube arrays up to 220 μm in linght: use in water photoelectrolysis and dye-sensitized solar cells"* Nanotechnology 18, Pennsylvania,USA, 2007.

[14]. A.G. Kontos, A.I. Kontos, D.S. Tsoulkleris, V. Likodimos, J. Kunze, P. Schmuki, *"Photo-induced effects on self-organized TiO_2 nanotube arrays: the influence of surface morphology"*, P. Falaras, Nanotechnology 20, Athens, Greece, 2009.

[15]. G.K. Mor, K. Shankar, M. Paulose, O.K. Varghese and C.A. Grimes, *"Enhaced photocleavage of water using titania nanotube arrays"*, Nano Letters 5, Pennsylvania, Usa, 2005.

[16]. J. Wang, Z. Lin, *"Anodic Formation of Ordered TiO_2 Nanotube Arrays: Effects of Electrolyte Temperature and Anodization Potential"*, J. Phys. Chem. C 113, Ames, Usa, 2009.

[17]. Z. Su, W. Zhou, *"Formation, microstructures and crystallization of anodic titanium oxide tubular arrays"*, J. Mater. Chem. 19 , St. Andrews, UK, 2009.

[18]. J.M. Macak, H. Hildebrand, U. Marten-Jahns, P. Schmuki, *"Mechanistic aspects and growth of large diameter self-organized TiO2 nanotubes"*, J. Electroanal. Chem. 621, Erlangen, 2008.

[19]. H. Kim, K. Lee, *"Dependence of the Morphology of Nanostructured Titanium Oxide on Fluoride Ion Content"*, Electrochem. Solid-State Lett. 12, Pohang, Korea, 2009.

[20]. N.F. Fahim, T. Sekino, M.F. Morks, T.Kusunose, *"Electrochemical growth of vertically-oriented high aspect ratio titania nanotubes by rabid anodization in fluoride-free media"*, J. Nanosci. And Nanotechnol. 9, Osaka, Japan, 2009.

[21]. O.K. Varghese, M. Paulose, K. Shankar, G.K. Mor, C.A. Grimes, *"Water-photolysis properties of micron-length highly-ordered titania nanotube-arrays"*, J. Nanosci. Nenotechnol. 5, Pennsylvania, USA, 2005.

[22]. Mura F., A. Masci, A. Pozio, M. Pasquali, "*Effect of a galvanostatic treatment on the preparation of highly ordered TiO_2 nanotubes"*, Electrochimica Acta 54, Rome, Italy, 2009.

[23]. Mor G.K., O.K. Varghese, M. Paulose, K. Shankar,C.A. Grimes, "*A review on highly ordered, vertically oriented TiO_2 nanotube arrays: Fabrication, material properties, and solar energy applications"* Sol. Energy Mat. & Sol. Cells 90, Pennsylvania, USA, 2006.

[24]. Elsanousi A., J. Zhang, H.M:H. Fadlalla, F. Zhang, H. Wang, X. Ding, Z. Huang, C. Tang *"Self-organized TiO_2 with controlled dimensions by anodic oxidation"* J. Mater. Sci. 43, Wuhan, China, 2008.

[25]. Q.A.S. Nguyen, Y.V. Bhargava, V.R. Radmilovic, T.M. Devine, *"Structural study of electrochemically synthesized TiO2 nanotubes via cross-sectional and high-resolution TEM"*, Electrochimica Acta 54, Berkeley, USA 2009.

[26]. R.J. Brook, *"Concise Encyclopaedia Of Advanced Ceramics Materials"*, Pergamon Press, Oxford, UK, 1991.

[27]. O.K. Varghese , D. Gong, M. Paulose, C.A. Grimes and E.C. Dickey, *"Crystallization and high-temperature structural stability of titanium oxide nanotube arrays"*, J. Mater. Res. 18, Pennsylvania. USA, 2003

[28]. .R. Hummer, P.J. Heaney, J.E. Post, *"Thermal expansion of anatase and rutile between 300 and 575 K using synchrotron powder X-ray diffraction"*, Powder Diffraction 22, Pennsylvania, USA, 2007.

[29]. R.R. Pawar, V.T. Deshpande, *"The Anisotropy Of the thermal expansion of α-Titanium"*, Acta Cryst. A24, Hyderabad, India, 1968.